

Fast-ion-induced erosion of leucine as a function of the electronic stopping power

A. Hedin, P. Håkansson, M. Salehpour,* and B. U. R. Sundqvist

Tandem Accelerator Laboratory, University of Uppsala, Box 533, S-751 21 Uppsala, Sweden

(Received 13 November 1986)

The fast-heavy-ion-induced neutral yield of intact molecules of the amino acid leucine has been determined as a function of the electronic stopping power, dE/dX . The experimental procedure is based on a collector method. The neutral yield varies approximately as $(dE/dX)^3$. A comparison of the neutral yield to the positive and negative ion-yield dependencies on stopping power, which are weaker, reflects the different mechanisms involved in ionization and desorption.

I. INTRODUCTION

Fast (MeV/amu) ions impinging on a solid target interact mainly with the electronic structure of the target material. As a result of the electronic energy deposition, target molecules in the surface region are desorbed as ions or neutral species (intact and fragmented). Desorbed ions were for the first time observed by Macfarlane *et al.* in 1974 (Ref. 1) and the effect was utilized as an ion source in a time-of-flight (TOF) mass spectrometer where the fast heavy ions were provided by a ^{252}Cf fission source.² The method is called plasma desorption mass spectroscopy (PDMS). It has so far been the most successful mass spectrometric technique for studies of large organic molecules.^{3,4}

For fundamental reasons and also from an applications point of view, it is important to understand the desorption and ionization mechanisms involved. Hitherto, most experimental work in this field has been aiming at measuring the secondary ion yield as a function of various primary ion parameters. The molecular ion yield, the number of desorbed secondary ions per incident primary ion, has been determined as a function of primary ion velocity,^{5,6} mass,^{5,7} charge state,^{8,9} angle of incidence,^{10,11} and electronic stopping power.¹²

Few measurements of neutral sputtering yields in the electronic stopping regime have been made so far. Some systems studied are water ice,^{13,14} UF_4 ,¹⁵ and frozen volatiles such as Xe (Ref. 16) and Ar.¹⁷ Recently, the first neutral yield of a biomolecule was presented. The yield of intact neutral molecules of the amino acid leucine was reported to be of the order of 1000 for 90-MeV ^{127}I ions.¹⁸ This implies that the yield of intact neutral molecules is about 10^4 times that of intact molecular ions. Since the desorption of neutrals dominates under the impact of a fast heavy ion, it is more relevant to study the neutral yield as a function of primary ion parameters when a deeper understanding of the desorption mechanisms is sought. This paper reports on a measurement of the neutral yield as a function of the electronic stopping power using a collector method similar to that used in Ref. 18.

II. EXPERIMENTAL PROCEDURE AND RESULTS

The principle of this experiment is the following: A target is irradiated with a beam of fast heavy ions. The

ejected charged and neutral species are collected on a silicon slice in front of the target. This will be referred to as the irradiation step, Fig. 1. The submonolayer amount of collected material is measured by moving the collector in vacuum to a plasma desorption mass spectrometer. The yield of molecular ions in this analysis step is a measure of the coverage of the collector and hence of the amount of ejected intact molecules in the irradiation. By varying the primary-ion species in the irradiation step, the dependence of total yield on the electronic stopping power can be obtained. The primary ions for both irradiation and analysis were provided by the Uppsala EN tandem accelerator. The vacuum in the experimental chamber was of the order of 10^{-6} Torr.

Both the target backing and the collector consist of rectangular (approximately $1 \times 10 \text{ cm}^2$) crystal plane cut silicon slices. They are movable in the vertical direction, perpendicular to the beam, so that several target and collector positions can be used in an experiment without breaking the vacuum. A collimator between the target and collector ensures that a well-defined collector position is utilized, avoiding transfer to adjacent positions. The target in this experiment consisted of the amino acid leucine (molecular weight of 131).

The principle of the mass spectrometer, discussed in detail elsewhere,² is presented in Fig. 2. ^{127}I ions of 78.2 MeV and of intensities of the order of 10^3 particles/s are used as primary ions. The primary ion is detected to initiate the time-of-flight measurement. The desorbed ions are accelerated and allowed to drift in a field-free region before detection. The PDMS spectra of a clean Si collector (a) and of the same collector having faced a leucine

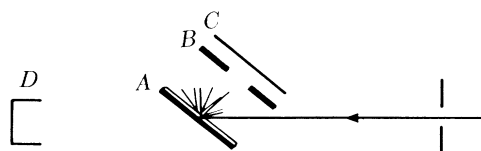


FIG. 1. The principle of the collector method. The primary ion impinges on the movable target (A). A collimator (B) ensures that the desorbed neutrals hit a well-defined spot on the movable collector (C). The Faraday cup (D) is used to monitor the beam current in the irradiations.

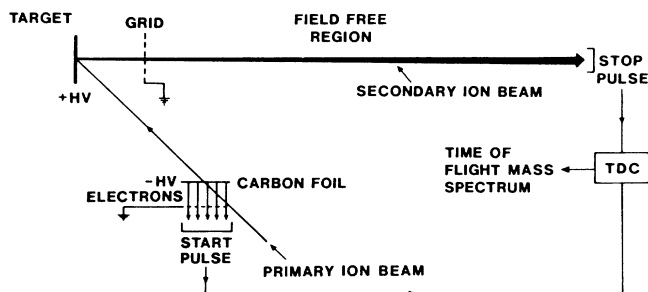


FIG. 2. The principle of PDMS-TOF. The primary ion is detected to initiate the TOF measurement. Secondary ions desorbed by the fast heavy ion impinging on the sample are accelerated and drift in a field-free region before detection.

target irradiated with 5×10^{10} 78.2-MeV ^{127}I ions (b) are shown in Fig. 3. The yield of molecular leucine ions, i.e., the number of detected leucine molecular $[M+H]^+$ ions (molecular weight of 132) per primary ion, is the measure of the collected amount. One may also note the presence of the fragment $[M-\text{COOH}]^+$ (molecular weight of 86) and cluster $[2M+H]^+$ (molecular weight of 263) ions.

A detailed description of the target and collector is given and some preliminary experiments to test the performance of the setup are discussed in the two following subsections.

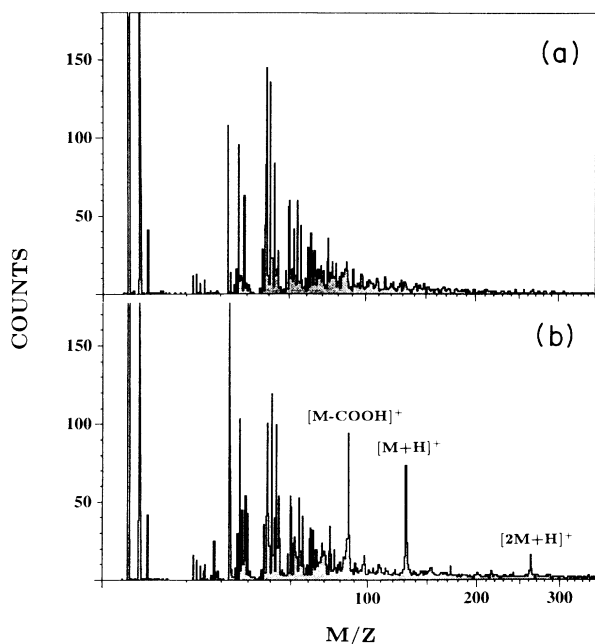


FIG. 3. PDMS spectra of a clean collector (a) and of one having faced a leucine target irradiated with 5×10^{10} 78.2-MeV ^{127}I ions (b). The same number of primary ions were used for the two spectra.

A. The target

The target was prepared by dissolving the sample molecules in a 4:1 mixture of acetic acid and trifluoroacetic acid to form a $10 \mu\text{g}/\mu\text{l}$ solution. The solution was electro-sprayed¹⁹ on the target backing to form a $\approx 100 \mu\text{g}/\text{cm}^2$ ($\approx 10^4 \text{ \AA}$) thick layer.

When the target is hit by a fast heavy ion, a certain area is damaged. In a first experiment this damage cross section, σ , was determined. The same target spot was irradiated with 78.2-MeV ^{127}I ions with interrupts for analysis. Several collector positions were used in order to avoid coverage of the collector (see below). The total amount of collected material as a function of the dose on the target is plotted in Fig. 4. The decrease in yield, Y , as a function of dose is described²⁰ by

$$Y = Y_0 e^{-N\sigma/A},$$

where Y_0 is the yield for an undamaged target, N the number of primary particles, and A the target area. The beam diameter is in this setup 2 mm and the angle of incidence 60° giving a target area of 6.3 mm^2 . The integrated yield, Υ , as a function of dose is thus

$$\Upsilon = Y_0 \frac{A}{\sigma} (1 - e^{-N\sigma/A}).$$

By fitting a function of this form to the data in Fig. 4 (solid line), a damage radius for the neutral yield of $44 \pm 10 \text{ \AA}$ was determined. This is close to the damage cross section for the molecular ion yield of leucine, $35 \pm 6 \text{ \AA}$.¹⁸ A target of the same thickness prepared with a more dilute ($2 \mu\text{g}/\mu\text{l}$) solution was also tested and no significant difference in neutral yield was obtained. The current densities in the irradiations in all experiments in this report were several orders of magnitude lower than what is needed for macroscopic heating of the target.

B. The collector

The collector silicon slices were etch cleaned by the following procedure:²¹ The slices are first washed in hydrofluoric acid and rinsed in distilled water. The washing is

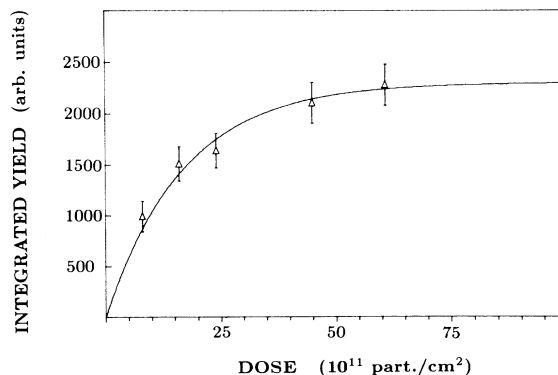


FIG. 4. Integrated yield as a function of dose on one target spot. The solid line is the expected function if the damage radius is 44 \AA .

repeated at 80°C in a solution of hydrochloric acid and hydrogen peroxide and finally in ammonium chloride and hydrogen peroxide. The sticking coefficient of the desorbed molecules to the collector is not known but this is not necessary as long as the sticking is constant since this is a relative measurement. It is however probably close to one, as discussed in Ref. 22. In a first test the collector was mildly contaminated by the breath of one of the experimentors (P.H.), and this did not alter the sticking significantly. In a subsequent test, another participant in the experimental work (A.H.) deliberately placed his thumb upon the etch-cleaned collector; this time a significant decrease in sticking resulted. When complete coverage of the collector is approached, the PDMS signal will no longer be proportional to the collected amount. In order to study this effect, the same collector spot was used to collect the ejecta from impacts of a large dose of 78.2-MeV ^{127}I primary ions. The irradiation was interrupted several times for analysis. Several target spots were used to avoid target damage. The result is shown in Fig. 5. As expected, the dependence is linear at low doses and saturates at higher doses. The coverage dose, N_0 , is defined as the primary irradiation dose which would cause coverage of the collector if there were no overlaps. This dose is obtained by fitting a function of the form $1 - e^{-N/N_0}$ to the data in Fig. 5 (solid line). N_0 was determined to 4×10^{11} for ^{127}I in our setup. This value is used to avoid coverage in the other experiments in this report and in the estimate of the average size of the sputtered particles in the following paragraph. The collector area used in each collection is approximately $10 \text{ mm} \times 5 \text{ mm}$.

From the reported value of the absolute yield,¹⁸ an estimate of the amount of collected material on a saturated collector can be made. This is interesting in order to determine the size of the ejected neutral particles. The presence of the leucine dimer molecule in the PDMS collector spectrum already at low coverage [Fig. 3(b)] indicates that part of the ejected material is in the form of small clusters. The result of this rough estimate is that

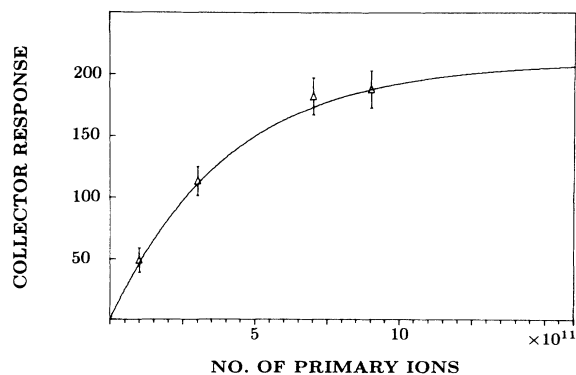


FIG. 5. The response of the collector, i.e., the yield of $[M+H]^+$ ions of leucine in the analysis, as a function of the desorbed amount expressed as the number of primary particles in the irradiation. The solid line is a function of the type $1 - e^{-N/N_0}$ from which a coverage dose is obtained.

saturation corresponds to between 1 and 3 monolayers, consistent with the possibility of part of the ejection being in the form of small clusters.

C. Yield versus electronic stopping power

As a fast heavy ion interacts with a target, the primary energy deposition is in excitations and ionizations close to the primary ion path. From the region of the primary energy deposition, the so-called infratrack defined by the infraradius, a distribution of secondary electrons is ejected into the ultratrack. The latter has a radius defined by the projected range of the most energetic secondary electrons. The desorbed molecules and molecular ions most likely originate from the ultratrack since the high-energy deposition in the infratrack is likely to damage the target molecules. The total secondary electron energy is proportional to the electronic stopping power of the primary ion. The infratrack and ultratrack radii are determined by the velocity of the primary ion. If the primary ion velocity is kept constant, the ultratrack energy density will hence be proportional to the electronic stopping power of the primary ion. A more detailed discussion on these processes is given in Ref. 23.

The following primary ions at a velocity of 1.11 cm/ns were used: 19.7-MeV ^{32}S , 33.7-MeV ^{58}Ni , and 78.2-MeV ^{127}I . The primaries penetrate a thin ($100 \mu\text{g}/\text{cm}^2$) carbon foil to reach charge-state equilibrium so that tabulated stopping-power values for the equilibrium state can be used. Several target and collector positions were utilized so as to avoid collector saturation and target damage as discussed previously. The whole experiment was carried out on one target and one collector slice without breaking the vacuum.

In an earlier version of the setup,²⁴ a new collector and target were inserted in the vacuum chamber for each primary ion species. The analysis was carried out with fission fragments from a ^{252}Cf source as primaries. This approach is more time consuming and is also sensitive to variations in quality between different targets and collectors. In that case, also 48.7-MeV ^{79}Br ions were used as primaries in the irradiation step. The measured yield values in the analysis in the two setups cannot be expected to agree in an absolute sense since different solid angles are involved in both the collection and the analysis. However, the dependence on stopping power should be the same in both cases.

The measured total yields of leucine in both experiments, normalized to that of ^{127}I ions are given in Table I together with the electronic stopping-power values, dE/dX , obtained from standard tables²⁵ and Bragg's rule.

TABLE I. Absolute yield of neutral molecules.

Primary ion	dE/dX [MeV/(mg/cm ²)]	M^0	
		Old setup	New setup
^{127}I	66.7	1200	1200
^{79}Br	50.9	410	
^{58}Ni	42.5	280	300
^{32}S	25.4	51	51

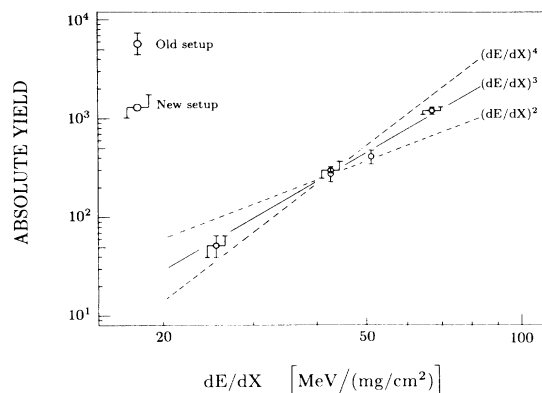


FIG. 6. The yield of neutral intact leucine molecules as a function of the electronic stopping power. Displaced error bars are data from the new setup, straight error bars from the old.

The absolute scale has been obtained using the figure for the absolute yield for ^{127}I given in Ref. 18. There, a $\cos\theta$ angular distribution for the neutral ejection and a sticking coefficient of one is assumed. A log-log plot of the yield as a function of dE/dX is given in Fig. 6. The error bars represent experimental reproducibility. Also plotted are the logarithmic least squares fits of the functions $(dE/dX)^n$ for $n=2, 3$, and 4 . The measured dependence of total yield on stopping power is closest to $(dE/dX)^3$. The dimer yield in the analysis is about 25% of that of the monomer independent of primary ion species in the irradiation and the degree of coverage of the collector. For an electrospayed thick target of leucine in PDMS, the dimer to monomer yield is roughly 50% for 78.2-MeV ^{127}I .

The yields of positive and negative molecular ions as a function of dE/dX were determined by directly inserting an electrospayed target of leucine in the mass spectrometer. Primary ions used in this case were 7.4-MeV ^{12}C , 9.9-MeV ^{16}O , 19.7-MeV ^{32}S , 48.7-MeV ^{79}Br , and 78.2-MeV ^{127}I . Also this experiment has been repeated and both data sets are presented in Table II and in Fig. 7 together with the neutral yields. The positive ion yield varies approximately linearly with dE/dX and the negative yield roughly as $(dE/dX)^2$.

III. DISCUSSION

As already mentioned, the presence of the leucine dimer in the PDMS spectra indicates that part of the desorbed

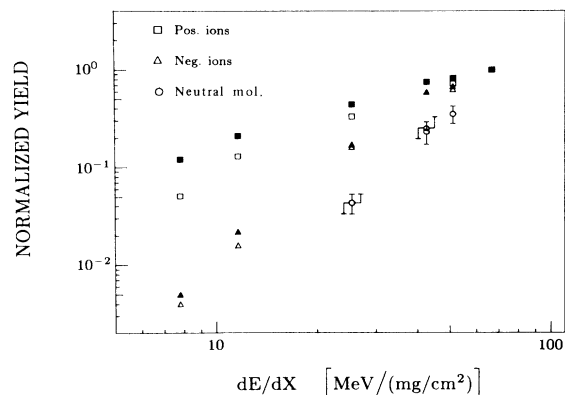


FIG. 7. Yield as a function of dE/dX . Circles are neutral data as in Fig. 6. Squares and triangles are positive and negative ion yields, respectively. Solid and open symbols represent two different experiments. All data sets have been normalized to one for the highest stopping-power value.

material is in the form of small clusters. Since the dimer to monomer yield is independent of primary ion species in the irradiation, the average cluster size is probably not strongly dependent on the primary ion. This result supports the reliability of the collector method used.

The intermolecular forces in electrospayed leucine are to a large extent hydrogen bonds. The fast heavy ion induced erosion of another hydrogen-bonded system of small molecules, namely of frozen water, has been studied extensively for fast light ions. The most highly ionizing primary ions, 1.6–25-MeV ^{19}F , have been used by Cooper *et al.*^{26,27} who found a faster than quadratic yield dependence.

The erosion of water ice in the electronic stopping-power regime has been reviewed by Johnson and Brown.¹⁴ They discuss a transition from a quadratic to a faster than quadratic dependence on dE/dX for the highest stopping-power values.^{26,27} The lowest stopping power in our measurements, that of ^{32}S , exceeds these values by about a factor of 2 so all our data would be in the fast scaling region.

The scaling is faster for negative ions than for positive. Both show saturation effects in that the yield increases more slowly for higher dE/dX values. Both these effects are in good agreement with what has been observed for similar systems¹² and interpreted in the ion track model.²³

TABLE II. Absolute yields of positive and negative molecular ions.

Primary ion	dE/dX [MeV/(mg/cm ²)]	$[M+H]^+$		$[M-H]^-$	
		Expt. 1	Expt. 2	Expt. 1	Expt. 2
^{127}I	66.7	0.13	0.29	0.13	0.043
^{79}Br	50.9	0.11	0.21	0.086	0.027
^{58}Ni	42.5	0.10		0.074	
^{32}S	25.4	0.059	0.096	0.021	0.0067
^{16}O	11.6	0.029	0.037	0.0028	0.00070
^{12}C	7.8	0.017	0.015	0.0006	0.00017

Since the yield of neutrals is about 10^4 times that of ions, the ionization mechanism presumably requires much more energy than the desorption mechanism. A molecule which is ionized has thus received substantially more energy than what is required for desorption, i.e., when the ionization energy condition is fulfilled, the desorption energy condition is automatically also fulfilled. Therefore, a model giving a good description of the ion yields may in fact only describe the ionization process and not the desorption.

This would be the case for the ion track model.²³ In this model, the major part of the secondary ionization occurs in the region of highest energy density close to the infratrack and all desorbed ions are assumed to originate from the surface. In a model for neutral desorption, much weaker processes and also depth dependencies will have to be included to account for the large yields.

In Fig. 7, it is noted that the reproducibility of the neutral measurements seems to be better than that of the molecular ions. This effect is probably related to problems with surface contaminants in the preparation and deposits from the pumping system in vacuum. The presence and relative amounts of surface contaminants may very well modify the interaction (bonding) to the surrounding molecules and thereby the desorption and ionization probabilities as discussed in Ref. 28. In fact, it is

often observed in our experiments on secondary ions, that the secondary ion yield changes with time in the high-vacuum (10^{-6} Torr) system. The ions most likely originate from the surface since ions from lower-lying layers would with high probability be neutralized before reaching the surface. Neutrals however, may to a large extent also come from lower layers and are therefore less sensitive to surface contaminations.

IV. CONCLUSIONS

The yield of neutral intact leucine molecules varies approximately as $(dE/dX)^3$. The scaling of molecular ions with dE/dX is slower. This is a reflection of the different processes involved in desorption and ionization. The depth profile of the neutral yield probably varies with dE/dX whereas ions predominantly originate from the surface. Neutral leucine molecules are to a large extent eroded in the form of small clusters. The damage cross section for the neutral ejection (44 Å) is close to that for molecular ion ejection. No satisfactory theoretical explanation of the neutral yield dependence on dE/dX has, as yet, been presented. Finding the solution to this problem is likely to be facilitated by more experimental data on neutral yield dependence on primary ion parameters.

*Present address: Argonne National Laboratory, CHM 200, 9700 South Cass Avenue, Argonne, IL 60439.

¹D. F. Torgerson, R. P. Skowronski, and R. D. Macfarlane, *Biochem. Biophys. Res. Commun.* **60**, 616 (1974).

²R. D. Macfarlane and D. F. Torgerson, *Int. J. Mass Spectrom. Ion Phys.* **21**, 81 (1976).

³B. Sundqvist, P. Roepstorff, J. Fohlman, A. Hedin, P. Håkansson, I. Kamensky, M. Lindberg, M. Salehpour, and G. Säve, *Science* **226**, 696 (1984).

⁴B. Sundqvist, I. Kamensky, P. Håkansson, J. Kjellberg, M. Salehpour, S. Widdiyasekera, J. Fohlman, P. A. Peterson, and P. Roepstorff, *Biomed. Mass Spectrom.* **11**, 242 (1984).

⁵P. Håkansson and B. Sundqvist, *Radiat. Eff.* **61**, 179 (1982).

⁶O. Becker, S. Della-Negra, Y. Le Beyec, and K. Wien, *Nucl. Instrum. Methods* **B16**, 321 (1986).

⁷B. Nees, E. Nieschler, N. Bischof, P. Dück, H. Fröhlich, W. Tiereth, and H. Voit, *Radiat. Eff.* **77**, 89 (1983).

⁸P. Håkansson, E. Jayasinghe, A. Johansson, I. Kamensky, and B. Sundqvist, *Phys. Rev. Lett.* **47**, 1227 (1981).

⁹E. Nieschler, B. Nees, N. Bischof, H. Fröhlich, W. Tiereth, and H. Voit, *Radiat. Eff.* **83**, 121 (1984).

¹⁰P. Håkansson, I. Kamensky, and B. Sundqvist, *Surf. Sci.* **116**, 302 (1982).

¹¹E. Nieschler, B. Nees, N. Gischolf, H. Fröhlich, W. Tiereth, and H. Voit, *Surf. Sci.* **145**, 294 (1984).

¹²P. Håkansson, I. Kamensky, M. Salehpour, B. Sundqvist, and S. Widdiyasekera, *Radiat. Eff.* **80**, 141 (1984).

¹³W. L. Brown, L. J. Lanzerotti, J. M. Poate, and W. M. Augustyaniak, *Phys. Rev. Lett.* **40**, 1027 (1978).

¹⁴R. E. Johnson and W. L. Brown, *Nucl. Instrum. Methods* **209/210**, 469 (1983).

¹⁵J. E. Griffith, R. A. Weller, L. E. Seiberling, and T. A. Tom-

brello, *Radiat. Eff.* **51**, 223 (1980).

¹⁶R. W. Ollerhead, J. Böttiger, J. A. Davies, J. L'Ecuyer, H. K. Haugen, and N. Matsunami, *Radiat. Eff.* **49**, 203 (1980).

¹⁷F. Besenbacher, J. Böttiger, O. Graversen, J. L. Hansen, and H. Sørensen, *Nucl. Instrum. Methods* **191**, 221 (1981).

¹⁸M. Salehpour, P. Håkansson, B. Sundqvist, and S. Widdiyasekera, *Nucl. Instrum. Methods* **B13**, 278 (1986).

¹⁹C. J. McNeal, R. D. Macfarlane, and E. L. Thurston, *Anal. Chem.* **51**, 2036 (1979).

²⁰M. Salehpour, P. Håkansson, and B. Sundqvist, *Nucl. Instrum. Methods* **B2**, 752 (1984).

²¹U. Jönsson, B. Ivarsson, I. Lundström, and L. J. Berghem, *Colloid Interface Sci.* **90**, 148 (1982).

²²Y. Qiu, J. E. Griffith, and T. A. Tombrello, California Institute of Technology Report Series BAP-31, 1982 (unpublished).

²³A. Hedin, P. Håkansson, B. Sundqvist, and R. E. Johnson, *Phys. Rev. B* **31**, 1780 (1985).

²⁴M. Salehpour, A. Hedin, P. Håkansson, and B. Sundqvist, Tandem Accelerator Laboratory Report No. TLU 138/86, 1986 (unpublished).

²⁵J. F. Ziegler, *Stopping Cross-Sections for Energetic Ions in All Elements* (Pergamon, New York, 1980).

²⁶B. H. Cooper, Ph.D. thesis, California Institute of Technology, 1981.

²⁷L. E. Seiberling, C. K. Meins, B. H. Cooper, J. E. Griffith, M. H. Mendenhall, and T. A. Tombrello, *Nucl. Instrum. Methods* **198**, 17 (1982).

²⁸G. P. Jonsson, A. B. Hedin, B. U. R. Sundqvist, B. G. S. Säve, P. F. Nielsen, P. Roepstorff, K.-E. Johansson, I. Kamensky, and M. S. L. Lindberg, *Anal. Chem.* **58**, 1084 (1986).